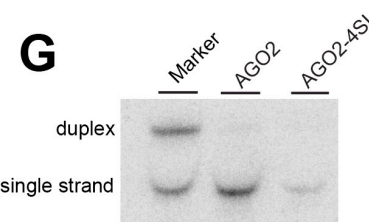
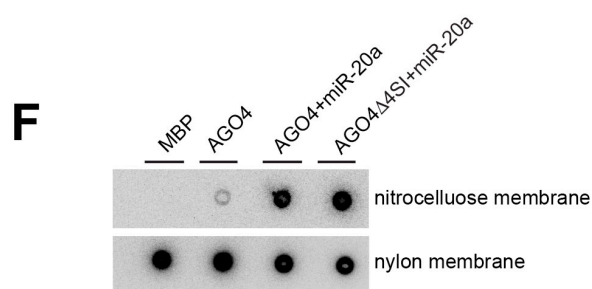
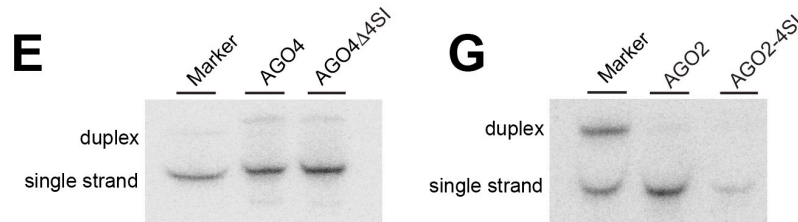
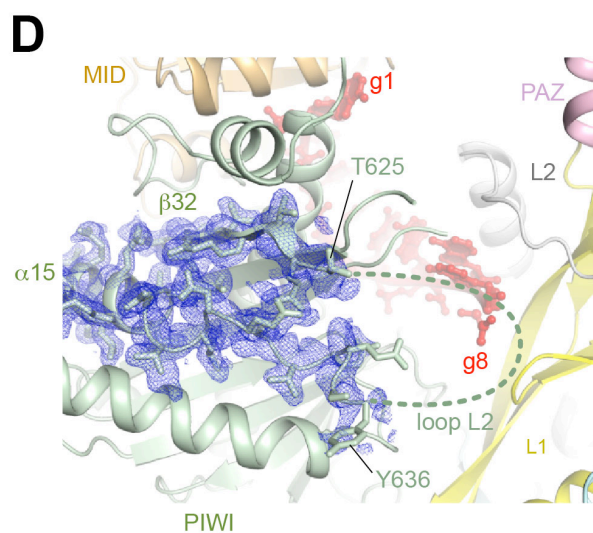
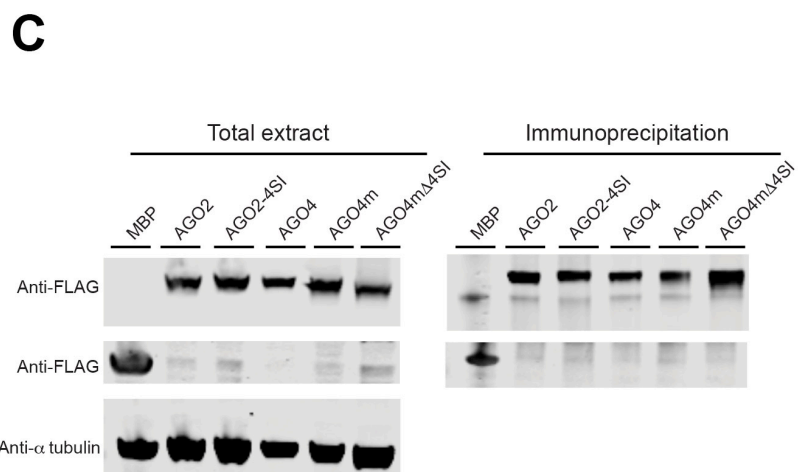
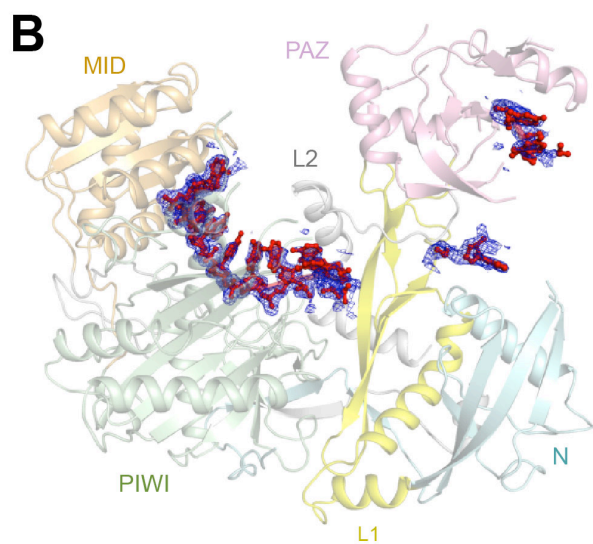
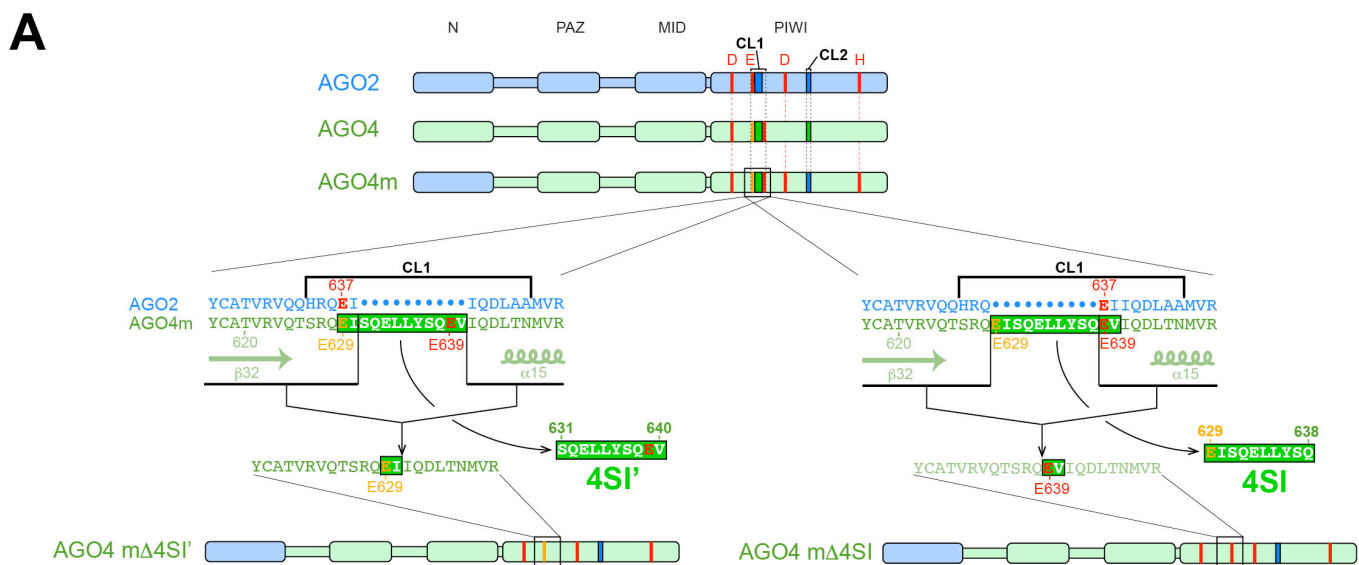


**Supplemental Information**

**Multidomain Convergence of Argonaute  
During RISC Assembly Correlates with  
the Formation of Internal Water Clusters**

**Mi Seul Park, Raul Araya-Secchi, James A. Brackbill, Hong-Duc Phan, Audrey C. Kehling, Ekram W. Abd El-Wahab, Daniel M. Dayeh, Marcos Sotomayor, and Kotaro Nakanishi**



**Figure S1. Strategy for making AGO4 into a catalytically active enzyme (Related to Figure 1)**

(A) Differences in the construct used by Hauptmann *et al.* (left) and that used in the current study (right), both of which generate a catalytically active AGO4 mutant.

(B) Simulated annealing  $F_o-F_c$  omit map contoured at  $2.5 \sigma$  (blue mesh) around the guide RNA. Colors as in Figure 1B.

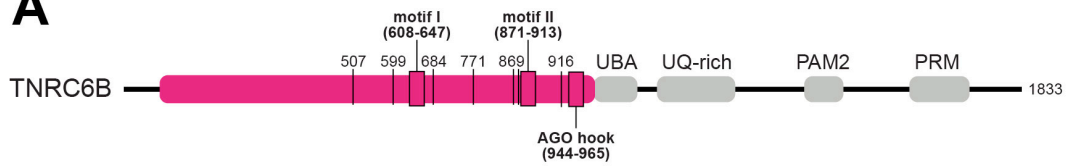
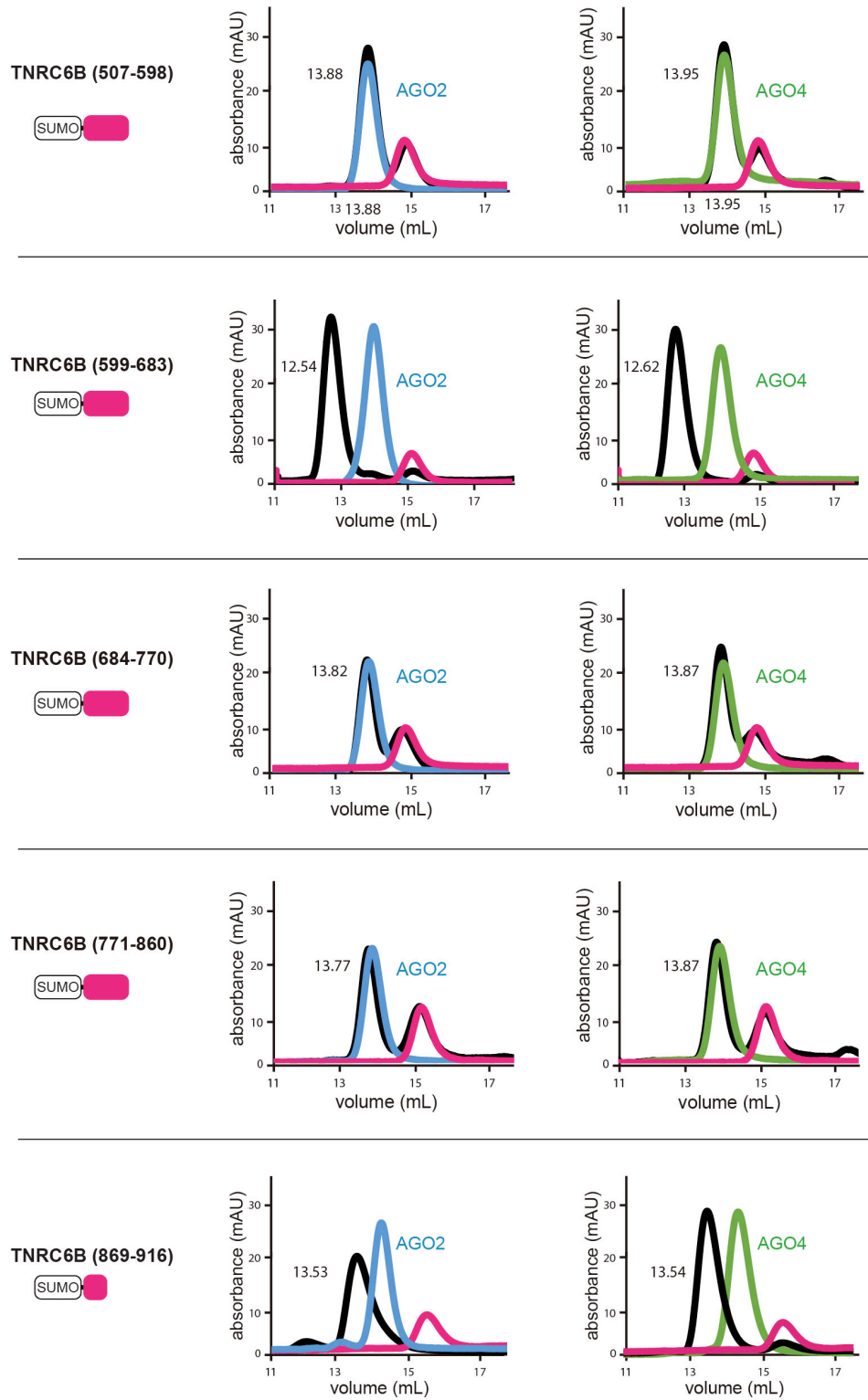
(C) FLAG-AGO2, FLAG-AGO4 and their mutants were expressed in HEK293T cells and detected with anti-FLAG antibody (left). Their protein amounts were adjusted based on the western blot (right) and used for target cleavage assay (Figure 1E).

(D) Simulated annealing  $F_o-F_c$  omit map contoured at  $2.2 \sigma$  (blue mesh) around  $\alpha 15$  and  $\beta 32$  of AGO4. The disordered loop L2, including 4SI, is depicted as dotted lines. Colors as in (B).

(E) RISC maturation assays of AGO4 and AGO4 $\Delta$ 4SI (Figure 1H and 1I). The lysates of HEK293T cells expressing either FLAG-AGO4 or FLAG-AGO4 $\Delta$ 4SI were adjusted by western blot so as to include 50 pmol of AGO, followed by incubation with miR-20a duplex. The duplex is composed of a 5' end labeled miR-20a and a fully complementary passenger strand that lacks a 5' monophosphate. After immunoprecipitation with anti-FLAG beads, the AGO-bound RNAs were extracted and resolved on 10% native gel.

(F) Filter binding assay of MBP, AGO4, and AGO4 $\Delta$ 4SI. The lysates of HEK293T cells expressing either FLAG-MBP, FLAG-AGO4 or FLAG-AGO4 $\Delta$ 4SI were incubated with miR-20a duplexes and then immunoprecipitated with anti-FLAG beads. After the AGOs were eluted from the beads with FLAG peptides, the AGOs were incubated with 60-nt 5' cap labeled mismatch targets. The resultants were spotted on a nitrocellulose membrane and a nylon membrane. AGO4 without miR-20a was used as a control to subtract the non-specific bound targets (Figure 1J).

(G) RISC maturation assays of AGO2 and AGO2-4SI (Figure 1K). The lysates of HEK293T cells expressing either FLAG-AGO2 or FLAG-AGO2-4SI were adjusted by western blot so as to include 50 pmol of AGO, followed by incubation with miR-20a duplex. The duplex is composed of a 5' end labeled miR-20a and a fully complementary passenger strand that lacks a 5' monophosphate. After immunoprecipitation with anti-FLAG beads, the AGO-bound RNAs were extracted and resolved on 10% native gel.

**A****B**

**Figure S2. Interactions of long TNRC6B fragments with AGO2 and AGO4 (Related to Figure 2)**

(A) Domain architecture of TNRC6B. Several long fragments were designed from the AGO-binding regions (pink) and expressed as SUMO-fused proteins.

(B) Gel filtration analyses of AGO2 (blue), AGO4 (green), SUMO-fused TNRC6B fragment (pink), and a mixture of a TNRC6B fragment with either AGO2 or AGO4 (black).

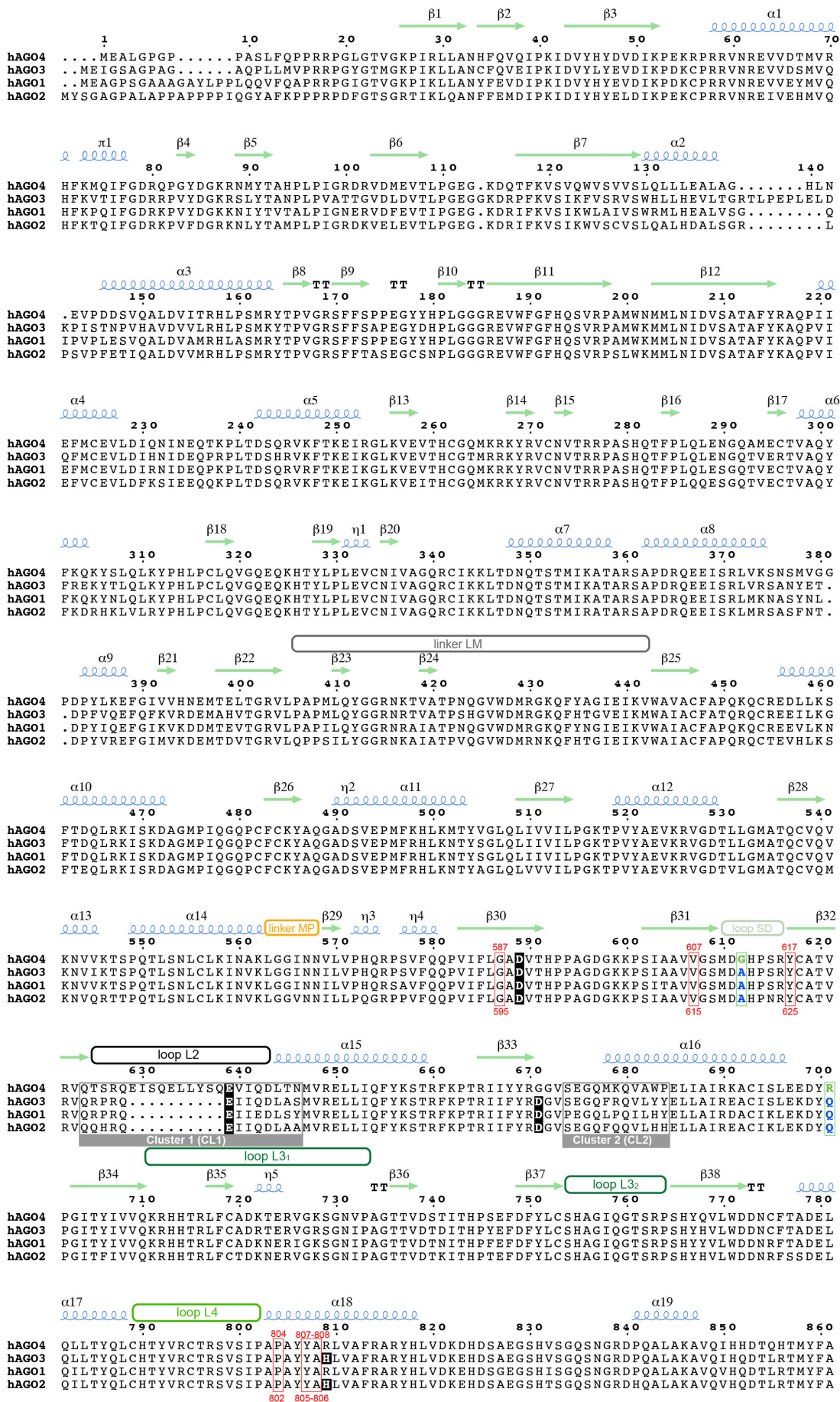


**Figure S3. Sequence alignment of human AGO paralogs (Related to Figure 2; Figure 3; Figure 4)**

Residue number and secondary structure of AGO4 are shown above the sequence. The four catalytic residues are highlighted with black columns. AGO4-specific residues in Trp Pocket-2 and -3 are boxed (green).

Residues involved in van der Waals interactions between two PIWI subdomains are boxed (red). Domain linkers and loops forming LAKE1 and LAKE2 are labeled above the sequence. CL1 and CL2 are boxed (gray).

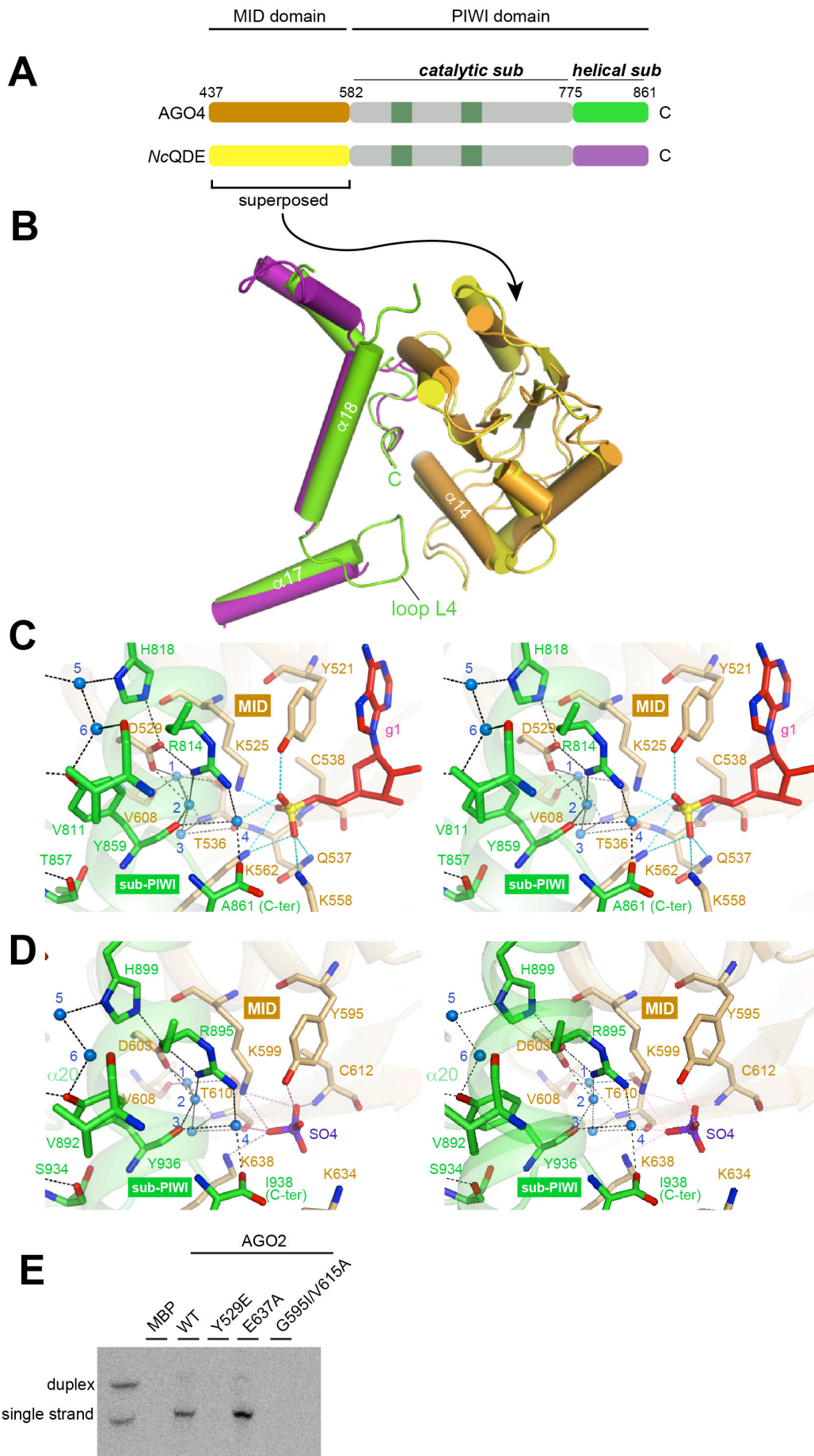




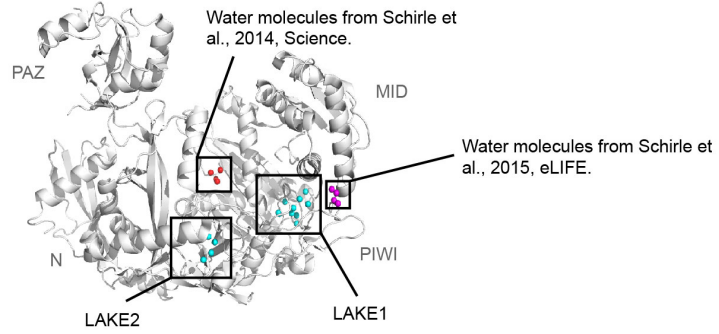
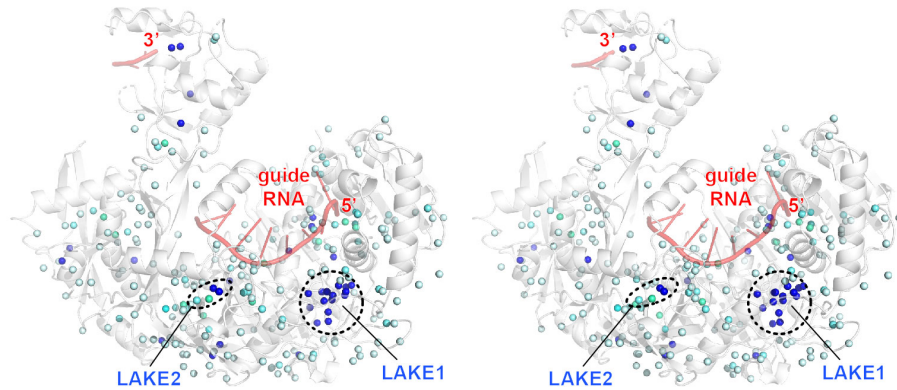
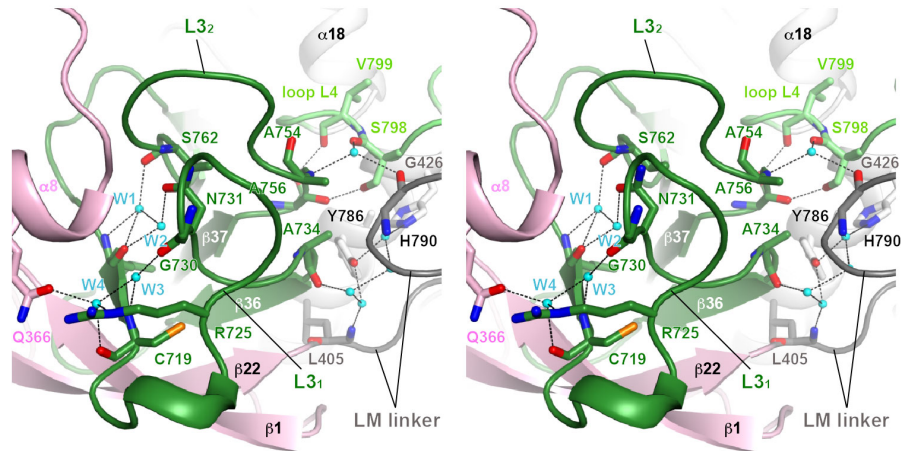
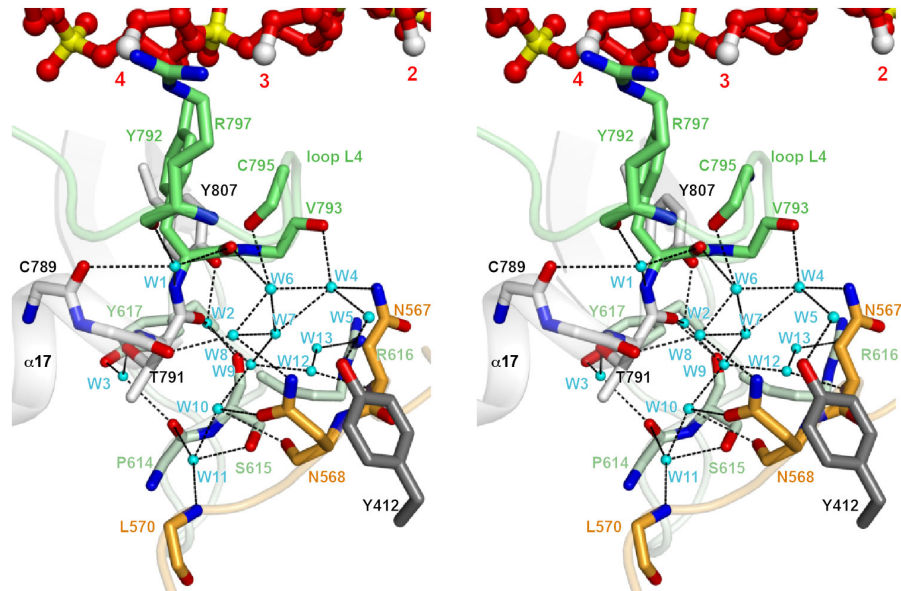
**Figure S4. Interactions between MID domain and PIWI-helical subdomain (Related to Figure 3; Figure 4)**

(A) MID-PIWI domain architectures of AGO4 and *NcQDE2*.

(B) Superposition of AGO4 and *NcQDE2* on their MID domains results in a good alignment of their PIWI-helical subdomains.

(C-D) Stereoviews of the interactions between the MID domain and PIWI-helical subdomain in AGO4 (C) and *NcQDE2* (D). Colors as in (A). Water molecules and hydrogen bonds are depicted as spheres (cyan) and dotted lines, respectively. For clarity, only g1 of the bound guide RNA is shown in (C). The bound sulfate ion is drawn as a stick model (magenta) in (D).

(E) A representative image of RISC maturation assay with siRNA duplex (Figure 3E).

**A****B****C****D**

**Figure S5. Water-mediated hydrogen-bonding network (Related to Figure 5)**

(A) Locations of LAKEs (cyan) and the previously reported water molecules at the active site (red) and the target nucleotide-1 pocket (magenta).

(B) Stereoview of water molecules bound to AGO4. The intensity of the blue color indicates the categories of the water molecule. Dark blue, cyan, and faint blue spheres indicate buried, cleft, and surface water molecules, respectively.

(C-D) Stereoview of the internal water-mediated hydrogen-bonding network in LAKE2 (C) and LAKE1 (D). Water molecules and hydrogen bonds are depicted as cyan spheres and dotted lines, respectively. The bound RNA in (D) is drawn as a ball-and-stick model. Colors as in Figure 4C.

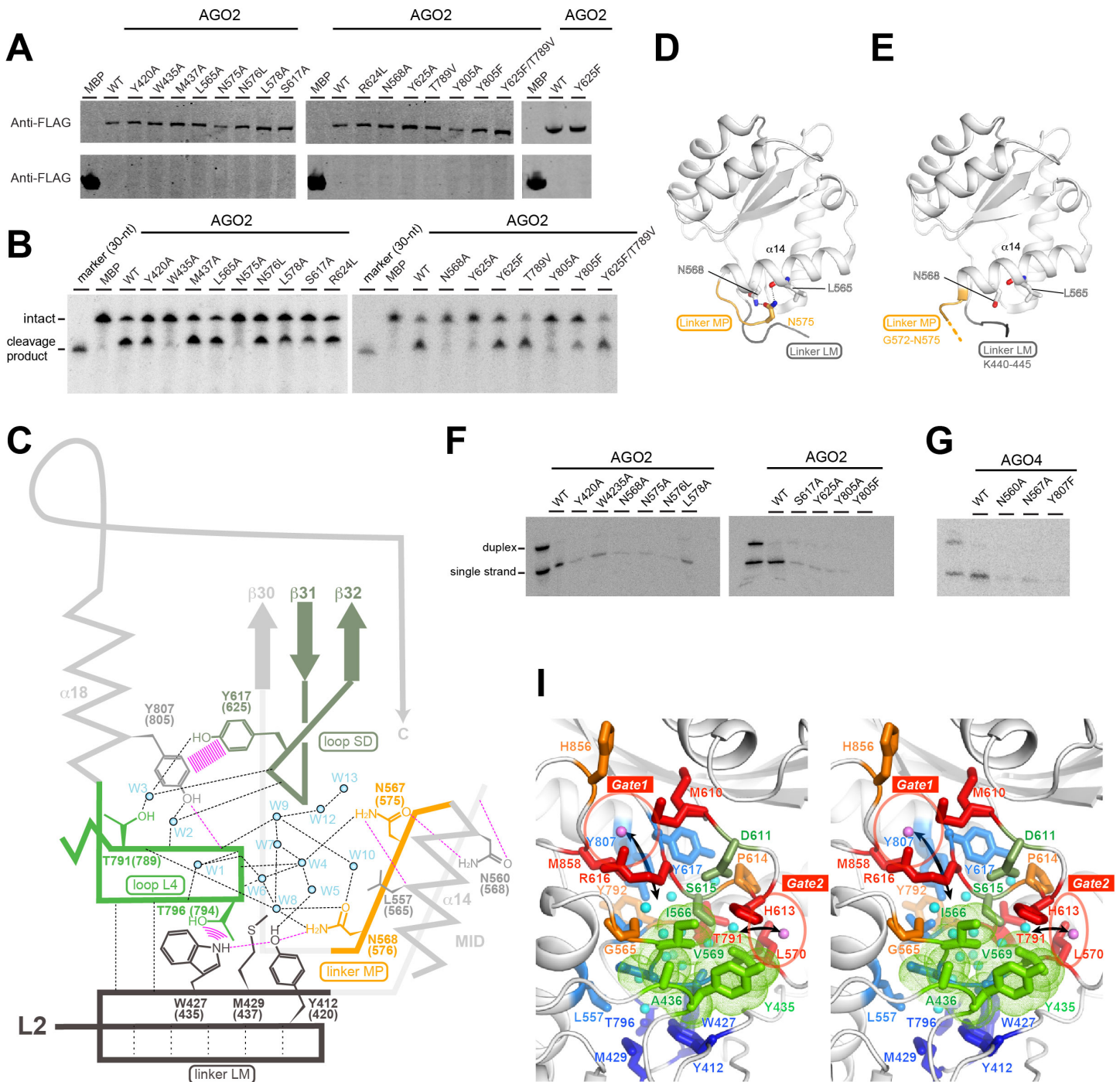


**Figure S6. Residues and their interactions required for LAKE1 formation (Related to Figure 5)**

(A) A representative image of western blot analysis with anti-FLAG antibody. Expression levels of mutants were tested, and the amount of proteins were adjusted for the target cleavage assay.

(B) A representative image of *In vitro* cleavage assay with miR-20a. All lysates were adjusted by western blots of (A) and the 5  $\mu$ M AGO proteins were incubated with 50 nM siRNA-like duplex of miR-20a for RISC assembly. 50 nM 5' cap-labeled target RNAs were used for the RNA cleavage reaction.

(C) A schematic of LAKE1. Conserved residues involved in the LAKE1 formation are shown. The internal water molecules and hydrogen bonds are depicted as spheres (cyan) and dotted lines (black), respectively. Hydrogen bonds not involving water molecules are colored in pink.

(D-E) Interactions between the MID domain and linker MP through two asparagine residues seen in the full-length AGO2 (D) (PDB ID: 4OLA) but not in the isolated AGO2 MID domain (E) (PDB ID: 3LUC).

(F-G) A representative image of RISC maturation assays with siRNA-like duplex of miR-20a (Figure 5H-5J).

(I) Stereoview of the two gates, Gate1 and Gate 2 (red circles), of the AGO4 LAKE1. Water molecules inside LAKE1 are colored in cyan. Two water molecules located just outside the two gates are colored in pink. Residues shaping the AGO4 LAKE1 can be categorized based on their roles; back wall (dark blue), middle wall (marine), gates (red), hydrophobic core (green), backbone (orange).

	560	570	580	590	600	610
hAGO4	NAKLGGINN	VLVPHQR	PSVFQQPVI	F <del>GL</del> ADVT	HPPAGDGK	KPSIAAVVGSMDG
hAGO3	NV <del>KL</del> GGINN	ILVPHQR	PSVFQQPVI	F <del>GL</del> ADVT	HPPAGDGK	KPSIAAVVGSMDA
hAGO2	NV <del>KL</del> GGVNN	ILLPQGR	PPVFQQPVI	F <del>GL</del> ADVT	HPPAGDGK	KPSIAAVVGSMDA
hAGO1	NV <del>KL</del> GGINN	ILVPHQR	SAVFQQPVI	F <del>GL</del> ADVT	HPPAGDGK	KPSITAVVGSMDA
DmAgo1	NV <del>KL</del> GGINS	ILVPSIR	PKVFNEPVI	F <del>GL</del> ADVT	HPPAGDNK	KPSIAAVVGSMDA
CeALG1	NV <del>KL</del> GGVNS	ILLPNVR	PRIFNEPVI	F <del>GL</del> CDLTH	PPAGDSRK	KPSIAAVVGSMDA
AtAG01	NV <del>KL</del> VGGRR	TVLVDALS	RRIPLVSDR	PTIIF <del>GL</del> ADVT	HPPHGEDS	SPSIAAVVGSQDWPEI
DmAub	NAKLMGAP	IQVVIPLH	GLMTVGF	DVCHSP	KNKNK	SYGAFVATMDQKES
DmPiwi	NCKLGKYP	MIELPLS	GLMTIGF	DI AKSTR	DRKR	AYGALIASMDLQON
BmAgo3	NCKLGGTL	WISISPFK	SAMIVGI	DSYHDP	SRRNR	SVCSFVASYNQSM
Miwi	MNCKMGGEL	WRVDMPLK	LAMIVGI	DCYHDT	TAGRR	SIAGFVASINEGM
DmAgo3	NCKLGGSL	WTVKIPFK	NVMIVGI	DSYHDP	SNRGN	SVAAFVASINSSY
Siwi	NCKLGGSP	WTVDIPLP	SLMVVGY	DVCHDTR	SKEK	SFGAFVATLDKQM
		655				
	620	630	640	650	660	
hAGO4	SRYCATV	RVQTSRQE	EISQELLYS	QEVIQDLT	NMVRELLIQFYKSTR	
hAGO3	SRYCATV	RVQRFRQ	EIIQDLA	SMVRELLIQFYKSTR		
hAGO2	NR <del>Y</del> CATV	RVQQHRQ	EIIQDLA	AMVRELLIQFYKSTR		
hAGO1	SRYCATV	RVQRFRQ	EIIEDLS	YMVRELLIQFYKSTR		
DmAgo1	SRYAATV	RVQQHRQ	EIIQELS	SMVRELLIMFYKSTGG		
CeALG1	SRYAATV	RVQQHRQ	EIISDLT	YMVRELLIQFYRNR		
AtAG01	TKYAGL	VCAQHRQ	ELIQDLF	KKEWKDPQ	KGVVTTGGMIKELLIAFRSTG	
DmAub	FRYFSTV	NEHIKGO	ELSEQMS	VNMACALRS	YQEQHR	
DmPiwi	STYFSTV	TECSAFD	VLANTLW	PMAKALRQY	QHEHR	
BmAgo3	TLWYSKV	IFQEKGO	EIVDGLK	CCLVDAL	THWYLRNSG	
Miwi	TRWFSRC	VFQDRGO	ELVDGLK	VCLQAAL	RAWSGCNE	
DmAgo3	SQWYSKA	VVQTKRE	EIVNGLS	ASFEIAL	KMYRKRNG	
Siwi	TOYYSIV	NAHTSGE	ELSSHMG	FNIASAV	KKFREKNG	
	670	680	690	700	710	
hAGO4	FKPTRI	IYR <del>RD</del> GV	SEGMKQ	VAWPELI	AIKACISLEEDYR	PGITYIVVQKRHHTR
hAGO3	FKPTRI	IYR <del>RD</del> GV	SEGFQ	RQVLYYELL	AIKACISLEEKDY	QPGITYIVVQKRHHTR
hAGO2	FKPTRI	IYR <del>RD</del> GV	SEGFQ	QVLHHELL	AIKACISLEEKDY	QPGITFIVVQKRHHTR
hAGO1	FKPTRI	IYR <del>RD</del> GV	SEGFQ	PQILHYELL	AIKACISLEEKDY	QPGITYIVVQKRHHTR
DmAgo1	YKPHRI	IYR <del>RD</del> GV	SEGFQ	PHVLQHELT	AIKACISLEEKDY	QPGITFIVVQKRHHTR
CeALG1	FKPARIV	VYR <del>RD</del> GV	SEGFQ	FNVLYYELR	AIKACISLEEKDY	QPGITFIVVQKRHHTR
AtAG01	HKPLRRI	IYR <del>RD</del> GV	SEGFQ	FYQVLLYELD	AIKACISLEEKDY	QPGITFIVVQKRHHTR
DmAub	SLFERIL	FFR <del>RD</del> GV	GDGQL	YQVNVSEV	NLTKDR	LDDEIYKSAGKQEGCRMTFIIVSKRINRSR
DmPiwi	KLERSR	IVFYR <del>RD</del> GV	VSSG	SLKQLF	EVDIEK	LKTEYARVQ.LSPPQLAYIVVTRSMNTR
BmAgo3	QLDRRI	IYR <del>RD</del> GV	GDGQL	KLQY	EIP	QMKICFTILGSNYQPTLTLYIVVQKRINTR
Miwi	YMP	SRVIVYR <del>RD</del> GV	GDGQL	KTLVNYEVP	QFLD	CLKSVGRGYNPRLTIVVKKRVNAR
DmAgo3	KLPTNII	IYR <del>RD</del> GV	GDGQL	LYTCLNYEIP	QFEMVC	GNRIKISYIVVQKRINTR
Siwi	TYPARIF	IYR <del>RD</del> GV	GDGQL	IPYVHSH	EVAEIK	KKLAEIY.AG.VEIKLAFIIVSKRINTR
	720	730	740	750	760	770
hAGO4	LF <del>CA</del> DKT	ER.VG	KSGNIP	PAGTV	DS <del>TI</del> THPSEF	DFYLC
hAGO3	LF <del>CA</del> DRTER	.VGR	SGNIP	PAGTV	DT <del>DI</del> THPYEF	DFYLC
hAGO2	LF <del>CA</del> TDKNER	.VG	KSGNIP	PAGTV	DT <del>TI</del> HTPTEF	DFYLC
hAGO1	LF <del>CA</del> DKNER	.IG	KSGNIP	PAGTV	DT <del>NI</del> THPFEF	DFYLC
DmAgo1	LF <del>CA</del> EKKEQ	.SG	KSNIP	PAGTV	DV <del>GI</del> THPTEF	DFYLC
CeALG1	LF <del>CA</del> VDKDDQ	.VG	KSNIP	PAGTV	DV <del>GI</del> THPTEF	DFYLC
AtAG01	LF <del>CA</del> QNHND	RRHSVDR	SGNIP	PAGTV	DS <del>KI</del> CHPTEF	DFYLC
DmAub	YFTGHR	NP	VPGTV	DDVITL	PERYD	DFLVSQ
DmPiwi	FFLNGQ	NPP	PGTIV	DDVITL	PERYD	DFLVSQ
BmAgo3	IFLKS	RDGY	DNP	PGTIV	DHCIT	TRRDWYDFLIVS
Miwi	IFFAQ	SGGRL	QNP	PGTIV	DVEVTR	PEWYDFLIVS
DmAgo3	IFSGS	GIHL	ENP	PGTIV	DQHIT	KSNTMYDFLIVS
Siwi	IFVQR	GRSG	ENP	PGTIV	DDVITL	PERYD
		797		818	827	
	780	790	800	810	820	830
hAGO4	CFTADEL	QLTYQL	CHTYVR	CTR	SVSIPAPAYY	ARLVAFRARYHLVDKDHDSDA
hAGO3	CFTADEL	QLTYQL	CHTYVR	CTR	SVSIPAPAYY	AHLVAFRARYHLVDKEHDSDA
hAGO2	RFSSDEL	QLTYQL	CHTYVR	CTR	SVSIPAPAYY	AHLVAFRARYHLVDKEHDSDA
hAGO1	RFTADEL	QLTYQL	CHTYVR	CTR	SVSIPAPAYY	ARLVAFRARYHLVDKEHDSG
DmAgo1	HFDSDEL	QLTYQL	CHTYVR	CTR	SVSIPAPAYY	AHLVAFRARYHLVEKEHDSG
CeALG1	NLTADEL	QLTYQ	MCHTYVR	CTR	SVSIPAPAYY	AHLVAFRARYHLVDREHDSG
AtAG01	NFTADEL	QLTYQ	MCHTYVR	CTR	SVSIPAPAYY	AHLAAFRARFYMEDRETSDSGSMASGSM
DmAub	GLNADK	LOML	SYKMT	MYN	YS	SGTIRVPAVCHYAHKLAFLVAESINRAP
DmPiwi	GLSPGK	MOKL	TYKMCH	LYY	NWS	GTRVPAVCOYAKKLATLVGTNLHSIP
BmAgo3	GITPDQ	CORL	TYKMCH	LYY	NWP	GTTRVPAVCOYAHKLSYLVGQCVHAQP
Miwi	GLKPDH	IQR	TYKLC	HLY	NWP	GVIRVPAVCOYAHKLAFLVGSIQHREP
DmAgo3	NYGPDII	OKL	SYKLC	CFLY	NW	AGTVRIPACCMYAHKLAFLYLGQSIQRD
Siwi	GLNPDRI	QR	TYKLT	HLTY	ENC	SSQVRVPSVCOYAHKLAFLAANSLHNQP
		856	858	850	860	
hAGO4	VSG	QSN	GRDPQALAKAV	QIH	HDTQHTMYFA	
hAGO3	VSG	QSN	GRDPQALAKAV	QIH	QDTLRTMYFA	
hAGO2	TSG	QSN	GRDQALAKAV	QVH	QDTLRTMYFA	
hAGO1	ISG	QSN	GRDPQALAKAV	QVH	QDTLRTMYFA	
DmAgo1	QSG	QSN	EDRTPGAMARAI	TVH	ADTKKVMYFA	
CeALG1	PSG	QSN	EDTTLSN	MARAV	QVHPDANNVMYFA	
AtAG01	ARGGG	MAGR	STRGPN	VNA	AVRPLPALKENVKRVMFYC	
DmAub					SAGLQNL	YFL
DmPiwi					QNALEK	KFYFL
BmAgo3					SDVL	VDKLFFL
Miwi					NLSL	NRLYYL
DmAgo3					AEAL	SEKLYFL
Siwi					HYSL	NETLYFL

**Figure S7. Sequence alignment of AGO- and PIWI-clade proteins (Related to Figure 7)**

Residues highlighted in red participate in the van der Waals interaction between two PIWI subdomains.

Residues in colored boxes (linker MP: orange, L3<sub>1</sub> and L3<sub>2</sub>: dark green, loop L4: bright green) have different properties between AGO and PIWI clades. Residue numbers of AGO4 and Siwi are shown above and below the sequence alignment, respectively. AGO-specific insert in L3<sub>1</sub> is colored in yellow (see Figure 7C-D).

Table S1. Detailed simulation statistics of LAKE1 and LAKE2 of AGO2<sub>cw</sub> and AGO4<sub>cw</sub> (Related to Figure 6)

AGO and Temp	Cavity	Number of water molecules						Avg. Occup.*	$t_1$ (ps)	$t_2$ (ps)
		Mean	SD	Variance	max	min	median			
AGO4 <sub>cw</sub> 300 K	LAKE1	10.3	1.8	3.2	18	5	10	10 ± 2	34.6	3.6
	LAKE2	7.3	1.6	2.7	18	3	7	7 ± 2	-	-
AGO4 <sub>cw</sub> 310 K	LAKE1	10.2	1.5	2.3	18	6	10	10 ± 2	31.4	3.2
	LAKE2	6.1	1.1	1.3	11	2	6	6 ± 1	-	-
AGO2 <sub>cw</sub> 300 K	LAKE1	12.7	1.4	2.1	19	8	13	13 ± 1	42.2	3.5
	LAKE2	4.7	0.8	0.6	8	2	5	5 ± 1	-	-
AGO2 <sub>cw</sub> 310 K	LAKE1	12.6	2.0	4.0	23	6	13	13 ± 2	25	2.8
	LAKE2	5.7	0.8	0.7	10	3	6	6 ± 1	-	-

\*Correspond to rounded up values of the mean ± sd number of water molecules in columns 3 and 4



Table S2. Details of simulated systems (Related to Simulation systems preparation section of STAR Methods)

System	#	PDB	$t_{\text{sim}}$ (ns)	Type	Ensemble	Temp (K)	Start	Size #atoms	Size (nm <sup>3</sup> )
AGO4cw	S1a	6OON	1.21	MinEQ	$NpT^*$	300	-----	164,443	12x12x12
AGO4cw	S1b	6OON	100	EQ	$NpT$	300	S1a	164,443	12x12x12
AGO4cw	S1c	6OON	100	EQ	$NpT$	310	S1a	164,443	12x12x12
AGO4ncw	S2a	6OON	1.21	MinEQ	$NpT^*$	300	-----	164,443	12x12x12
AGO4ncw	S2b	6OON	100	EQ	$NpT$	300	S2a	164,443	12x12x12
AGO4ncw	S2c	6OON	61	EQ	$NpT$	310	S2a	164,443	12x12x12
AGO2cw	S3a	4OLA	1.21	MinEQ	$NpT^*$	300	-----	164,230	12x12x12
AGO2cw	S3b	4OLA	100	EQ	$NpT$	300	S3a	164,230	12x12x12
AGO2cw	S3c	4OLA	100	EQ	$NpT$	310	S3a	164,230	12x12x12

Summary of all MD simulations. Asterisk (\*) denotes simulations that consisted of 5000 steps of minimization, 200 ps of dynamics with the backbone of the protein restrained ( $k_{\text{bbr}} = 1 \text{ kcal mol}^{-1} \text{ \AA}^{-2}$ ), and 1 ns of free dynamics in the  $NpT$  ensemble ( $\gamma = 1 \text{ ps}^{-1}$ ).

Table S3. Primer list (Related to Cloning, expression, and purification of AGO proteins and TNRC6B fragment section of STAR Methods)

Oligonucleotides	Source	Identifier
AGO2G595I/V615A-FW- CAGCAGCCCGTCATCTTTCTGATAGCAGACGTCAC, CCATTGCCGCCGTGGCGGGCAGCATGGACGCC	This paper	N/A
AGO2G595I/V615A-RV - GGCGTCCATGCTGCCCCGCCACGGCGGCAATGG, GGCGTCCATGCTGCCCCGCCACGGCGGCAATGG	This paper	N/A
AGO2Y420A-FW- GCCGCCCTCCATCCTCGCCGGGGGCAGGAATAAAG C	This paper	N/A
AGO2Y420A-RV - GCTTTATTCTGCCCCGGCGAGGATGGAGGGCGG C	This paper	N/A
AGO2W435A-FW- CCCTGTCCAGGGCGTCGCGGACATGCGGAACAAG CAGT	This paper	N/A
AGO2W435A-RV - ACTGCTTGTTCCGCATGTCCGCGACGCCCTGGACA GGG	This paper	N/A
AGO2L565A-FW- CAGACCCTGTCCAACCTCTGCGCGAAGATCAACGT CAAGCTGGGA	This paper	N/A
AGO2L565A-RV - TCCCAGCTTGACGTTGATCTTCGCGCAGAGGTTGG ACAGGGTCTG	This paper	N/A
AGO2N568A-FW- GTCCAACCTCTGCCTGAAGATCGCCGTC	This paper	N/A
AGO2N568A-RV - CGCCTCCAGCTTGACGGCGATCTTCAGGCA	This paper	N/A
AGO2N575A-FW- GTCAAGCTGGGAGGCGTGGCCAAC	This paper	N/A
AGO2N575A-RV - CTGGGGCAGCAGGATGTTGGCCACGCCTCCC	This paper	N/A
AGO2 L578A -FW- CTGGGAGGCGTGAACAACATCGCGCTGCCCCAGG GCAGG	This paper	N/A
AGO2 L578A -RV - CCTGCCCTGGGGCAGCGCGATGTTGTTACGCCTC CCAG	This paper	N/A
AGO2S617A -FW- CCGCCGTGGTGGGCGCCATGGACGCCACCCC	This paper	N/A
AGO2S617A -RV - GGGGTGGGCGTCCATGGCGCCCACCACGGCGG	This paper	N/A
AGO2Y625A -FW- CGCCCACCCCAATCGCGCCTGC	This paper	N/A
AGO2Y625A -RV - CGCACGGTGGCGCAGGCGCGATTGGG	This paper	N/A
AGO2Y805A-FW-TCCCAGCCAGCATACGCCGCTC	This paper	N/A
AGO2Y805A-RV - GGCCACCAGGTGAGCGGCGTATGCTGGCG	This paper	N/A
AGO2-4SI-FW- TGCAGCAGCACCGGCAGGAGATCTCCCAAGAGCTC CTCTACAGTCAAGA	This paper	N/A
AGO2-4SI-RV - GCGGCCAGGTCTTGATGATCTCTTGAAGTAGAG GAGCTCTTGG	This paper	N/A

AGO4m-FW- GACTTCCCGGCAGGAGATCTCCAAGAGCTCCTCT ACAGTCAAGA, GACTTCCCGGCAGGAGATCTCCAAGAGCTCCTCT ACAGTCAAGA, GGAGGGGTATCTGAGGGACAATTCCAGCAGGTTCT CCACCACGAGTTGCTGGCCATCCGTG	This paper	N/A
AGO4m-RV - AACCATGTTAGTCAGGTCCTGGATGACCTCTTACT GTAGAGGAGCTCTTGG, CTTGCCCTAAATGCTACAAGATGGGCATAATATGCA GGGGC, GGCCGGTAATCTTCTTCCAATTGATACAGGCCTCA CGGATGGCCAGCAACT	This paper	N/A
AGO4mΔ4SI-FW- GTGCAGACTTCCCGGCAGGAGGTCATCCAGGACCT GACTAA	This paper	N/A
AGO4mΔ4SI-RV- TTAGTCAGGTCCTGGATGACCTCCTGCCGGGAAGT CTGCAC	This paper	N/A
TNRC6B-599-683-FW- GCGCGCCTCGAGTCAGAGCTCCCCCATCCAGA	This paper	N/A
TNRC6B-599-683-RV- GCGCGCGGATCCGATTGTCAGGCTGTCTTGCAGA	This paper	N/A
TNRC6B-507-598-FW- GCGCGCGGATCCTCTCAGGGAGAATGGAAACAGC	This paper	N/A
TNRC6B-507-598-RV- GCGCGCCTCGAGTCAAGGATGTGTGGGCCTGTACG	This paper	N/A
TNRC6B-684-770-FW- GCGCGCGGATCCTCAGCCTCTACAGAGTGGAAGA CC	This paper	N/A
TNRC6B-684-770-RV- GCGCGCCTCGAGTCAAGACACAGGTTTACTTGCAG AACTTTC	This paper	N/A
TNRC6B-771-860-FW- GCGCGCGGATCCGGGTGGGGTGAAGGAGGG	This paper	N/A
TNRC6B-771-860-RV- GCGCGCCTCGAGTCACTCCAGCTGGAATTGGAAGG	This paper	N/A
TNRC6B-869-916-FW- GCGCGCGGATCCACTGTGGATAATGGTACTTCAGC ATG	This paper	N/A
TNRC6B-869-916-RV- GCGCGCAAGCTTTCAGGGTTCCCCCAGCTGG	This paper	N/A
TNRC6B-616-636-FW- CAAATTAAGCAGGACACAGTGTGGTACTCGAGTCT GGTAAAGAAACCG	This paper	N/A
TNRC6B-616-636-RV- CGGTTTCTTTACCAGACTCGAGTCACCACACTGTGT CCTGCTTAATTTG	This paper	N/A
TNRC6B-623-636-FW- ACAGAGAACAGATTGCTGCATCCTGGGGCCAAACT CAAATTAAGC	This paper	N/A
TNRC6B-623-636-RV- GCTTAATTTGAGTTTGGCCCCAGGATGCAGCAATCT GTTCTCTGT	This paper	N/A
TNRC6B-617-634-FW- GCGCGCGGATCCGTGCTCTCAAACACTGGCTGGG	This paper	N/A
TNRC6B-617-634-RV-GCGCGCCTCGAGTCA AATGTCCCACTGTGTCCTGC	This paper	N/A

TNRC6B-617-634(Q625E)-FW- TCAAACACTGGCTGGGGCGAAACTCAAATTAAGCA GGACACAGTGT	This paper	N/A
TNRC6B-617-634(Q625E)-RV- ACACTGTGTCCTGCTTAATTTGAGTTTCGCCCCAGC CAGTGTTTGA	This paper	N/A
TNRC6B-617-634(K629A)-FW- GCTGGGGCCAAACTCAAGCTAAGCAGGACACAGTG TGGGA	This paper	N/A
TNRC6B-617-634(K629A)-RV- TCCCACACTGTGTCCTGCTTAGCTTGAGTTTGGCCC CAGC	This paper	N/A
TNRC6B-617-634(Q630R)-FW- GGGGCCAAACTCAAATTAAGCGGGACACAGTGTGG GACATTTGA	This paper	N/A
TNRC6B-617-634(Q630R)-RV- TCAAATGTCCCACACTGTGTCCCGCTTAATTTGAGT TTGGCCCC	This paper	N/A